https://doi.org/10.5194/egusphere-2026-3436
Preprint. Discussion started: 30 June 2026

Temperature stabilization using Stratospheric Aerosol Injections minimises drying over Africa only when combined with a strong decarbonization effort

Temitope S. Egbebiyi[1,2,3*], Temitope S. Fafure[1], Daniele Visioni[2], Romaric C. Odoulami[1], Babatunde J. Abiodun[3,4], Simone Tilmes[5], Chris Lennard[3], Mark New[1]

[1]African Climate and Development Initiative, University of Cape Town, South Africa
[2]Department of Earth and Atmospheric Sciences, Cornell University, Ithaca, NY, USA.
[3]Climate System Analysis Group, Environmental and Geographical Science Department, University of Cape Town, South Africa
[4]Nansen-Tutu Centre for Marine Environmental Research, Department of Oceanography, University of Cape Town, South Africa
[5]NSF National Centre for Atmospheric Research, Boulder, Colorado, USA

Correspondence to: Temitope S. Egbebiyi (temitope.egbebiyi@uct.ac.za); Romaric Odoulami (romaric.odoulami@uct.ac.za)

Abstract. Climate change poses severe risks to African agriculture, water resources, and ecosystems. Temperature overshoot scenarios, in which global warming temporarily exceeds target thresholds such as 1.5 or 2.0°C before declining through mitigation and carbon removal later in the century, are plausible future trajectories. Yet, their regional impacts and the reversibility of changes during the overshoot remain poorly characterized. Stratospheric aerosol injection (SAI) has been proposed as a means to limit peak warming during overshoot; however, its effects on African climate extremes and water availability require careful assessment. This study analyses different CESM2-WACCM6 simulations to evaluate changes in temperature extremes, precipitation patterns, and surface moisture budget across Africa, using two baseline scenarios, the high GHG forcing scenario (SSP5-8.5) and the SSP5-3.4-OS overshoot scenario, which includes strong decarbonization and carbon removal efforts after 2040. In addition, three SAI intervention scenarios are assessed, targeting 1.5 and 2.0°C (for the overshoot scenario, only) above pre-industrial levels. We compute selected ETCCDI-based climate indices, including Growing Degree Days, Warm Spell Duration Index, Consecutive Dry Days, and precipitation intensity metrics for baseline and overshoot (2060-2079) periods. Our results reveal near-universal, statistically significant changes (> 90%) in temperature indices during overshoot, with 5-30% increases depending on the metric. Precipitation indices exhibit more heterogeneous responses, with 40-80% of the area showing significant changes. SAI interventions consistently reduce temperature-related indices across Africa, with the strongest cooling effects in tropical regions. However, precipitation responses to SAI display substantial spatial heterogeneity and scenario dependency: West Africa's Sahel shows increased moisture availability under high SAI compared to SSP5-8.5, Central Africa exhibits mixed responses with regional drying in parts of the Congo Basin, and East Africa demonstrates a dipole pattern of coastal wetting and interior drying that intensifies at higher warming thresholds. All these changes are magnified under high-cooling scenarios (using the high forcing baseline) compared with cooling under overshoot, in which case many precipitation differences are reduced.

https://doi.org/10.5194/egusphere-2026-3436
Preprint. Discussion started: 30 June 2026

1 Introduction

African agriculture remains highly dependent on rainfall, with approximately 95% of the continent's cropland lacking irrigation and 55 to 62% of the sub-Saharan workforce employed in the sector (Trisos et al., 2022). Rainfed agriculture is vital for food production, as it is the primary economic activity, contributing to approximately 15% of the Gross Domestic Product (GDP) of most African countries (Mupangwa et al., 2016; Ofori et al., 2021). This dependence on rainfall renders agricultural productivity, food security, and rural livelihoods highly sensitive to variations in precipitation timing, intensity, and seasonal distribution (Sultan & Gaetani, 2016). Observed warming across Africa has been approximately 0.5°C over the past half-century, with the rate of increase accelerating in recent decades (Almazroui et al., 2020). For example, CMIP6 projections under high emission pathways indicate continental warming of 1.8°C in the near future (2030-2059) to 4.4°C by the late 21st century (2070-2099) under SSP5-8.5, accompanied by spatially heterogeneous shifts in precipitation that include drying over northern and southern Africa and wetting over central and eastern regions (Almazroui et al., 2020). These climatic shifts carry profound consequences for African agriculture, which is highly rainfed. Changes in the frequency and intensity of extreme events, including prolonged droughts, intense rainfall episodes, and extended warm spells, pose direct threats to crop yields, water availability, and ecosystem services (Klutse et al., 2018; Sylla et al., 2016). Agroclimatic indices and their changes under different scenarios can be used to characterise crop-climate interactions, which influence agricultural production through changes in growing season length, as well as the timing of planting and harvesting (Chemura et al., 2022; Egbebiyi et al., 2025).

The Expert Team on Climate Change Detection and Indices (ETCCDI) framework provides standardised metrics for quantifying such extremes, including consecutive dry days, precipitation intensity, and warm spell duration (Peterson, 2005). Previous analyses using these indices over West Africa have shown that temperature extremes are projected to intensify. In contrast, precipitation extremes exhibit marked regional heterogeneity (Klutse et al., 2018), with implications that extend across the continent. Current emission trajectories suggest that global temperatures will likely exceed key warming thresholds such as 1.5°C and 2.0°C above pre-industrial levels before stabilising at lower targets through aggressive mitigation and carbon dioxide removal (O'Neill et al., 2016). Such a warming pathway, often referred to as temperature overshoot, is exemplified by the CMIP6 SSP5-3.4-OS pathway, which follows the high-forcing SSP5-8.5 trajectory until 2040, after which strong mitigation and decarbonization measures produce a peak in surface temperature between 2060-2080 and a subsequent decline in global temperatures (Tilmes et al, 2020; Tebaldi et al., 2021). The transient period of elevated warming during overshoot may trigger irreversible impacts on ecosystems, even if end-of-century temperatures eventually return to target levels (Boucher et al., 2012). Despite the policy relevance of overshoot scenarios, their regional climate impact, particularly over Africa, remain poorly characterised. Hence, there is a need to understand how temperature overshoot affects agroclimatic indices and their implications for rainfed agriculture, particularly crop production, which is crucial for developing adaptive strategies.

https://doi.org/10.5194/egusphere-2026-3436
Preprint. Discussion started: 30 June 2026

Stratospheric aerosol injection (SAI), a proposed solar radiation modification technique involving the sustained release of sulfur dioxide into the stratosphere to form reflective aerosol particles, has emerged as a potential complementary strategy to limit peak warming during overshoot periods (Tilmes et al., 2016; MacMartin et al., 2018; Tilmes et al., 2020). By increasing planetary albedo and reflecting incoming shortwave radiation, SAI could theoretically reduce the magnitude and duration of temperature exceedances above desired thresholds (MacMartin et al., 2017; Kravitz et al., 2017). Recent modelling studies using feedback-controlled injection algorithms have demonstrated that SAI can maintain global mean surface temperatures at specified temperature targets while simultaneously managing interhemispheric and pole-to-equator temperature gradients (Richter et al., 2022; Tilmes et al., 2020). However, most targets used in those simulations are related to global or zonal mean surface temperatures, whereas the regional climate responses to SAI over Africa are complex and remain an active area of investigation. Previous studies examining SAI impacts on African climate have revealed substantial spatial heterogeneity in precipitation responses, with potential reductions in Sahel monsoon rainfall (Da-Allada et al., 2020), mixed effects on temperature and precipitation extremes in South Africa (Patel et al., 2023), and region-dependent changes in extreme precipitation patterns across the continent (Quagraine et al., 2025). Pinto et al. (2020) demonstrated that Africa's climate response to SRM is characterised by differential regional sensitivity. While SRM significantly reduces mean and extreme temperatures across the continent, its effect on precipitation is less linear and varies markedly across different parts of Africa, particularly between East and West Africa (Pinto et al., 2020; Egbebiyi et al., 2025). For example, Egbebiyi et al. (2025) showed that relative to SSP5-8.5, SAI using G6sulfur may lead to a decrease in total annual rainfall and very heavy rainfall in the region, notably in the Central, West and East African zones. In addition, the study further revealed that under a high-emission scenario, SAI intervention relative to SSP5-8.5 may lead to an increase in the Growing Season Length (GSL) across African regions except over Madagascar (MDG), Central Africa (CEAF), with a projected decrease (Egbebiyi et al., 2025). A recent comprehensive assessment by Kumi et al. (2025) further highlighted that Africa's climate response depends critically on the characteristics of the SAI strategy. These studies collectively underscore the need for targeted assessments of how SAI interacts with specific emission pathways and warming trajectories, particularly under overshoot conditions that represent increasingly plausible future scenarios. However, no study has investigated the combined effects of temperature overshoot and SAI on agroclimatic indices and the surface moisture budget over Africa, and the present study addresses this gap.

Here, we analyze CESM2-WACCM6 simulations to evaluate changes in ETCCDI-based agroclimatic indices across Africa under two baseline scenarios, the SSP5-3.4-OS overshoot scenario (with aggressive mitigation and CDR after 2040, leading to a rapid decline in CO_2 concentrations in the second half of the century) and the high-forcing SSP5-8.5 scenarios as a reference. The SAI intervention scenarios were simulated to maintain temperatures at 1.5°C above pre-industrial levels for both baseline scenarios and 2.0°C for the overshoot scenario only. We further assess the surface moisture budget over the key monsoonal regions of West, Central, East, and Southern Africa. This gap is particularly significant given that the peak warming period during overshoot may represent a critical window of vulnerability for African agriculture and water

https://doi.org/10.5194/egusphere-2026-3436
Preprint. Discussion started: 30 June 2026

resources. Our analysis addresses three questions: (1) How do temperature and precipitation extremes change during the overshoot period relative to warming threshold baselines and a strong cooling SAI scenario under the high forcing scenario? (2) How effectively does SAI moderate these changes, and how do the effects vary regionally? (3) What are the implications for the surface moisture budget in monsoon regions in Africa (West, Central, Southern, and East Africa)?

2. Data and Methodology

2.1 Study Area

The study focuses on the African continent (approximately 35°S to 38°N, 20°W to 55°E), a region particularly vulnerable to climate change impacts on agriculture, water resources, and ecosystems (Fig. 1). This study covers the African continent and Madagascar, spanning hydro-climatic gradients from the Mediterranean/North African zone through the Sahara–Sahel arid transition, the humid equatorial Congo Basin, and the subtropical climates of southern Africa. These contrasts are primarily governed by the seasonal migration of the ITCZ/ITD, the dynamics of the West African Monsoon (WAM), and key circulation features such as the African Easterly Jet (AEJ), which together regulate moisture transport, convection, and rainfall seasonality across tropical Africa (Cook, 1999; Nicholson, 2013; Arias et al., 2021). To enable robust sub-continental interpretation and to avoid continent-wide averaging that can mask localized signals, the African domain was stratified into five geo-political sub-regions as depicted in Figure 1: North Africa (NAF), West Africa (WAF), Central Africa (CAF), East Africa (EAF) and Southern Africa (SAF). This regionalization is the widely used IPCC-style climate reference region, which group areas of broadly similar climate characteristics to support consistent intercomparison across models and scenarios (Iturbide et al., 2020; Arias et al., 2021). This region-based framing is especially important for crop-climate applications because suitability responds non-linearly to regional differences in thermal stress, rainfall seasonality, and moisture availability. Accordingly, crop suitability patterns and scenario-driven changes are evaluated at both continental and sub-regional scales to identify geographically concentrated hotspots of improvement or degradation, consistent with recent Africa-focused assessments of climate intervention implications for agricultural suitability (Egbebiyi et al., 2025). A land mask derived from model topography data is applied to exclude ocean grid cells from the analysis.

https://doi.org/10.5194/egusphere-2026-3436
Preprint. Discussion started: 30 June 2026

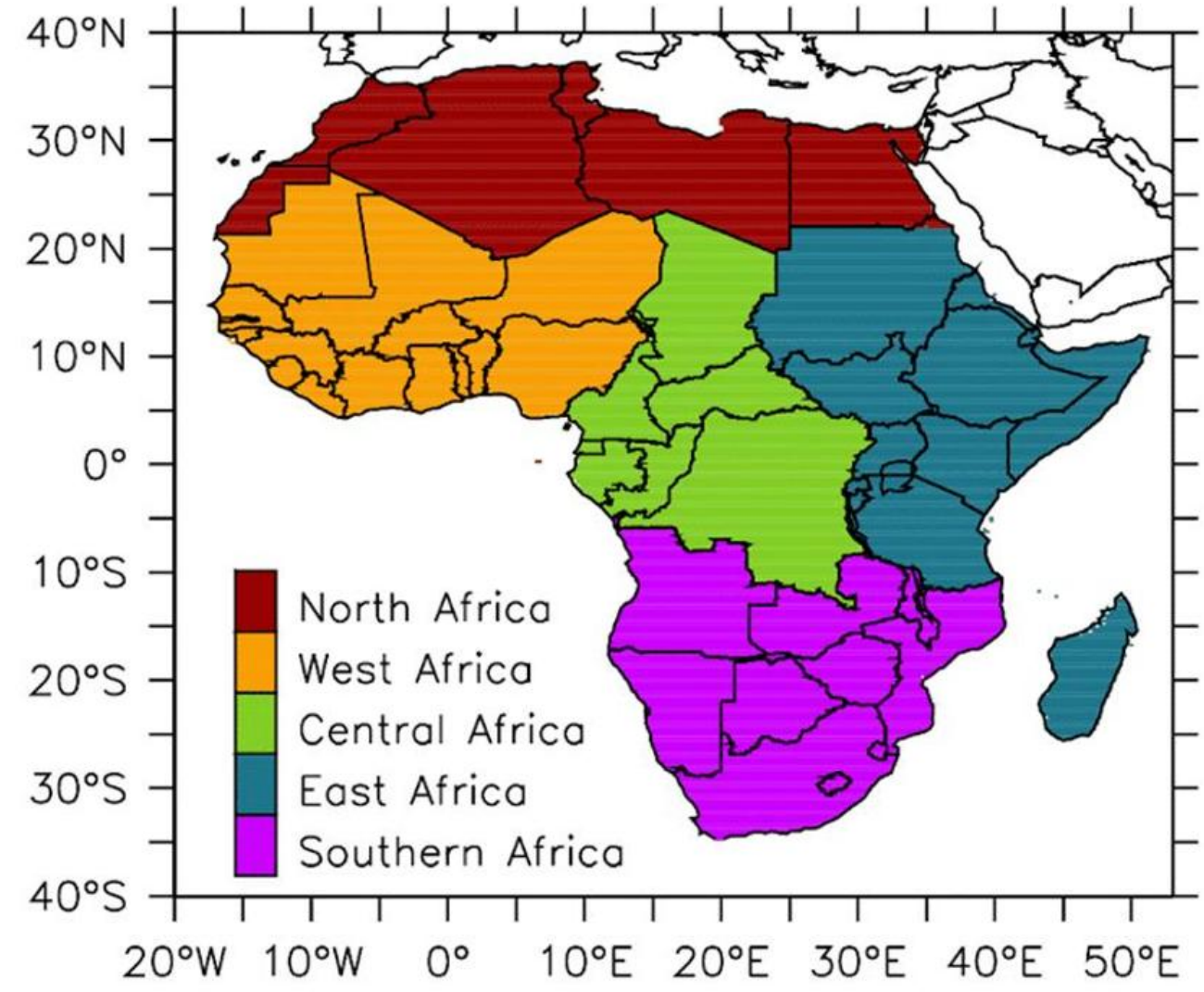

Figure 1: The study area showing African geo-political sub regions North Africa (NAF), West Africa (WAF), Central Africa (CAF), East Africa (EAF), Northeast Africa (NEAF), Southern Africa (SAF).

2.2 Model Description

This study utilises climate model output from the Community Earth System Model version 2 (CESM2) with the Whole Atmosphere Community Climate Model version 6 (WACCM6) atmospheric component. CESM2-WACCM6 is a state-of-the-art Earth system model that has contributed to the Coupled Model Intercomparison Project Phase 6 (CMIP6) (Eyring et al., 2016; Danabasoglu et al., 2019; Gettelman et al., 2019). The WACCM6 atmospheric model uses a horizontal resolution

https://doi.org/10.5194/egusphere-2026-3436
Preprint. Discussion started: 30 June 2026

of 1.25° in longitude and 0.95° in latitude, with 70 vertical layers extending to approximately 150 km altitude (6×10^{-6} hPa). The model includes comprehensive tropospheric, stratospheric, mesospheric, and lower thermospheric chemistry (Emmons et al., 2019) and uses a modal aerosol scheme (MAM4) for both troposphere and stratosphere (Liu et al., 2016). The atmospheric model is coupled to several other components, including the Parallel Ocean Program version 2 (POP2), the Community Ice Sheet Model version 2.1 (CISM2.1), the Community Land Model version 5 (CLM5), and the sea-ice model CICE 5.1.2 (Danabasoglu et al., 2019).

2.3 Experimental Design and Scenarios

The analysis employs simulations based on the CMIP6 Shared Socioeconomic Pathway 5-3.4-Overshoot (SSP5-34-OS) scenario as the baseline, following the experimental design described by Tilmes et al. (2020). This scenario follows the high forcing SSP5-8.5 pathway until 2040, after which strong mitigation efforts and carbon dioxide removal are implemented, producing a temperature overshoot above desired targets before eventual decline (O'Neill et al., 2016). The stratospheric aerosol geoengineering (SAG) experiments utilise a feedback control algorithm to maintain global mean surface temperatures at specific targets-1.5°C and 2.0°C above pre-industrial (1850-1900) levels-by adjusting sulfur dioxide injection rates at four stratospheric locations (30°N, 15°N, 15°S, and 30°S) at 5 km above the tropopause (MacMartin et al., 2017; Kravitz et al., 2017). In addition to global mean temperature, the algorithm maintains interhemispheric and pole-to-Equator temperature gradients to minimise side effects, including overcooling in the tropics and reduced polar warming (Tilmes et al., 2018). Three primary scenarios are analysed:

(1) SSP5-34-OS: The baseline overshoot scenario without geoengineering intervention.

(2) Geo SSP5-34-OS 1.5: SAG intervention maintaining temperatures at 1.5°C above pre-industrial.

(3) Geo SSP5-34-OS 2.0: SAG intervention maintaining temperatures at 2.0°C above pre-industrial.

For comparison, additional simulations using the high forcing SSP5-8.5 scenario are included to assess the dependency of impacts on baseline greenhouse gas concentrations and injection amounts. Two analysis frameworks are employed based on warming threshold exceedance, which are **1.5°C Threshold Analysis; b**aseline period defined as years when global mean surface temperature first reaches 1.5°C above pre-industrial (approximately 2020-2025 in WACCM6), compared with the overshoot period (2060-2079). Also, **2.0°C Threshold Analysis; b**aseline period defined as years when global mean surface temperature first reaches 2.0°C above pre-industrial (approximately 2034 in WACCM6), compared with the overshoot period (2060-2079). A summary of the model description and scenarios can be found in Table 1.

https://doi.org/10.5194/egusphere-2026-3436
Preprint. Discussion started: 30 June 2026

Table 1: Overview of Model Simulations

Model	Experiment	Pathway	Accum. SO_2	Max SAT
WACCM6	SSP5-85	SSP5-85	0	6.3°C
WACCM6	SSP5-34-OS	SSP5-34-OS	0	3.0°C
WACCM6	Geo SSP5-85 1.5	SSP5-85	~1665 Tg	1.5°C
WACCM6	Geo SSP5-34-OS 1.5	SSP5-34-OS	~599 Tg	1.5°C
WACCM6	Geo SSP5-34-OS 2.0	SSP5-34-OS	~317 Tg	2.0°C

2.4 Methods

2.4.1 Climatic Indices

In this study, the Expert Team on Climate Change Detection and Indices (ETCCDI) Peterson (2002) was employed to estimate changes in agro-climatic indices that influence agricultural production. Daily model output of reference height temperature (TREFHT) and total precipitation (PRECC + PRECL, representing convective and large-scale precipitation) were analyzed. From these primary variables, a suite of climate indices following ETCCDI standards relevant for agricultural production in Africa was computed using the xclim Python library (Bourgault et al., 2023). The list and definition of these indices can be found in Table 2.

https://doi.org/10.5194/egusphere-2026-3436
Preprint. Discussion started: 30 June 2026

Table 2: The Expert Team on Climate Change Detection Indices (ETCCDI) indices used to analyse agro-climatic indices

Index	Indicator	Definitions	Unit
CDD	consecutive dry days	maximum number of consecutive days with RR < 1 mm	days
CWD	consecutive wet days	maximum number of consecutive days with RR ≥ 1 mm	days
R1MM	number of wet days	annual count of days when PRCP≥ 1mm	mm
R20MM	number of heavy precipitation days	annual count of days when PRCP≥ 20mm	mm
SDII	simple daily intensity index	average precipitation amounts on wet days (days with at least 1 mm of precipitation)	mm/day
PRCPTOT	annual total wet day precipitation	annual total precipitation in wet days (RR ≥ 1 mm)	Mm
T_{mean}	Mean Temperature	Annual mean temperature	ºC
GDD	Growing Degree Days	Accumulated thermal units above a base temperature of 10°C, representing heat accumulation for crop development	°C-days
GDDI	Growing Degree Days Intensity	Annual GDD/Number of days with Tmean > 10°C	°C/days
OGD	Optimum Growing Days	Annual count of days where 10°C ≤ Tmean ≤ 35°C	days
WSDI	Warm Spell Duration Index	Annual count of days with at least six consecutive days when the maximum temperature exceeds the 90th percentile of the reference period (days).	days

180

https://doi.org/10.5194/egusphere-2026-3436
Preprint. Discussion started: 30 June 2026

2.4.2 Surface Moisture Budget

The surface moisture budget, expressed as the difference between precipitation and evapotranspiration (P minus ET), is computed to assess regional water availability under each scenario. Evapotranspiration (ET, in mm day^{-1}) is derived from the model latent heat flux (LHFLX, in W m^{-2}) following:

$$ET = \frac{LHFLX \times 86400}{\rho_w \times L_v} \quad (1)$$

where L_v = 2.5 × 10^6 J kg^{-1} is the latent heat of vaporisation, ρ_w= 1000 kg m^{-3} is the density of water, and 86400 is the number of seconds per day. P minus ET is computed at each land grid cell for every ensemble member, with positive values indicating a moisture surplus (precipitation exceeds evapotranspiration) and negative values indicating a moisture deficit. The analysis focuses on four African monsoonal regions: West Africa (WAF; 4°N to 18°N, 18°W to 15°E), Central Africa (CAF; 10°S to 8°N, 8°E to 27°E), East Africa (EAF; 12°S to 12°N, 27°E to 52°E), and Southern Africa (SAF; 35°S to 10°S, 8°E to 42°E). For each region, P and ET are masked to land grid cells and aggregated using area weighting with cos(latitude) factors before averaging across ensemble members. Annual P minus ET time series, seasonal climatology (DJF, MAM, JJA, SON), and baseline versus overshoot period means (2060 to 2079) are then derived. For the SSP5-3.4-OS scenarios, which branch from SSP5-8.5 in 2040, the baseline period (2015 to 2034) is drawn from the SSP5-8.5 simulations because the two pathways are identical before that year.

2.4.3 Statistical Analysis

Changes between the baseline and overshoot periods are computed as simple differences for each climate index. Statistical significance of changes is assessed at each grid cell using Welch's t-test (unequal variances t-test), which compares the ensemble distributions of baseline and overshoot period means between scenarios without assuming equal variances. Grid cells are considered to show statistically significant changes where $p < 0.05$. Ensemble means values are computed from 3 ensemble members for each scenario, and spatial patterns of change are visualized on maps with stippling marking grid cells that are not statistically significant. To summarize detectability across indices and scenarios, the percentage of African land area exhibiting statistically significant changes is calculated as the number of significant land grid cells divided by the total number of land grid cells, multiplied by 100. These percentages are displayed as a heatmap with climate indices arranged on the vertical axis (temperature related indices grouped above precipitation indices) and the four scenarios on the horizontal axis, where colour intensity indicates the fraction of land area showing significant changes for each metric and scenario pair.

3. Results

3.1 Temperature and precipitation changes under unmitigated and overshoot pathways

The temporal evolution of the temperature and precipitation indices illustrates divergence between scenarios in Africa (Fig. 2). Under SSP5-8.5, mean temperature, Growing Degrees Days (GDD) intensity, and Warm Spell Duration Index (WSDI)

https://doi.org/10.5194/egusphere-2026-3436
Preprint. Discussion started: 30 June 2026

increase continuously through 2099, while under SSP5-3.4-OS, these indices plateau begin to decline after approximately 2060-2080, reflecting the onset of the recovery phase. Precipitation indices: total annual precipitation (PRCPTOT), consecutive wet days (CWD) and Simple Daily Intensity Index (SDII), show greater inter-ensemble variability and less clear separation between the two scenarios compared to temperature indices (Fig. 2).

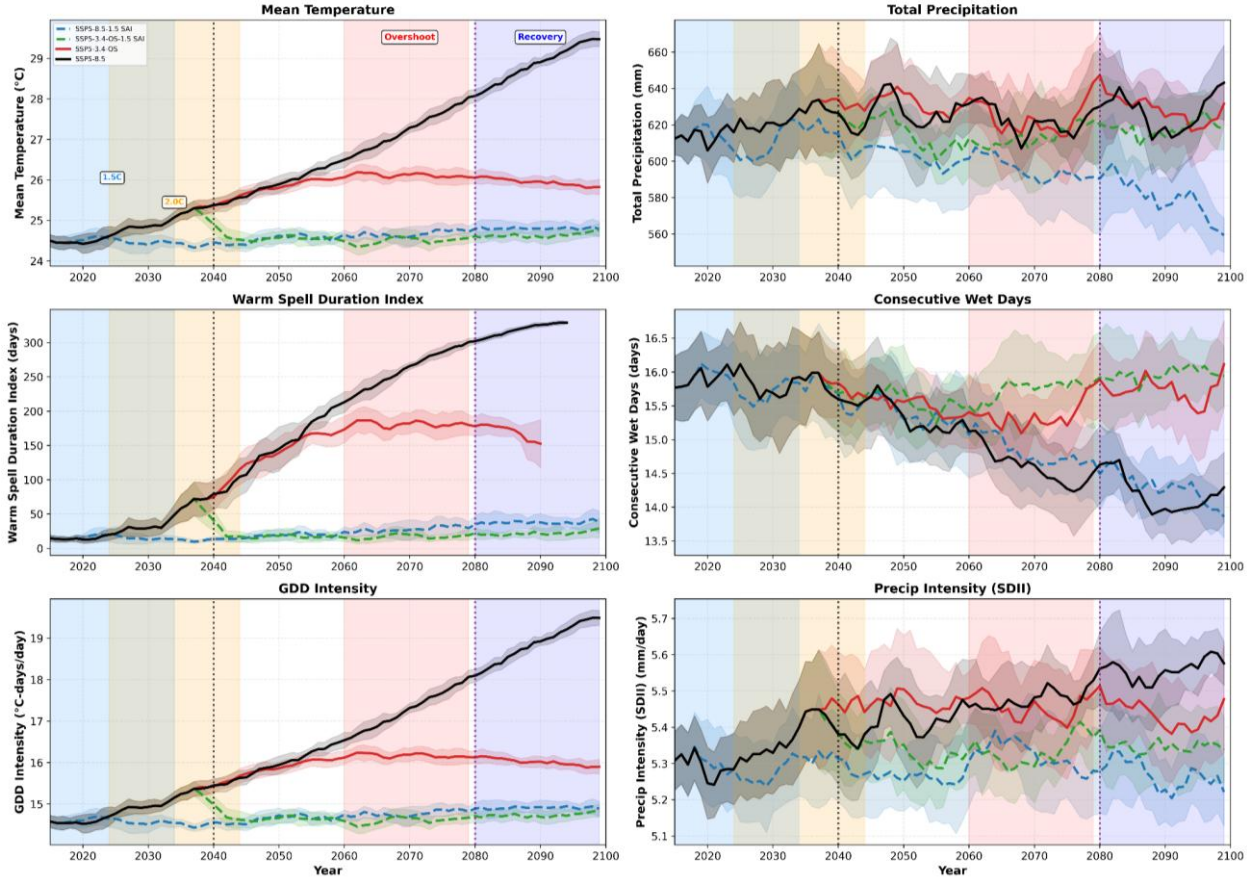

Figure 2: Time series of selected climate indices averaged over Africa (2015 to 2099). Left column: Mean Temperature, Warm Spell Duration Index, GDD Intensity. Right column: Total Precipitation, Consecutive Wet Days, Precipitation Intensity (SDII). Lines represent 5-year centred running means of ensemble mean values; shading denotes ±1 standard deviation across ensemble members. Red shading marks the overshoot period; blue shading marks the recovery period.

The variability in the precipitation indices is consistent with the lower statistical significance identified in the spatial analysis (Fig. 3). The baseline versus overshoot comparison across combined thresholds (Fig. A1) confirms that temperature indices show the largest and most consistently significant percentage changes (Fig. A2) relative to the baseline, while precipitation indices exhibit smaller and more variable changes. However, these continent-mean trajectories conceal substantial regional heterogeneity, which the spatial analysis (Fig. 3) makes visible.

https://doi.org/10.5194/egusphere-2026-3436
Preprint. Discussion started: 30 June 2026

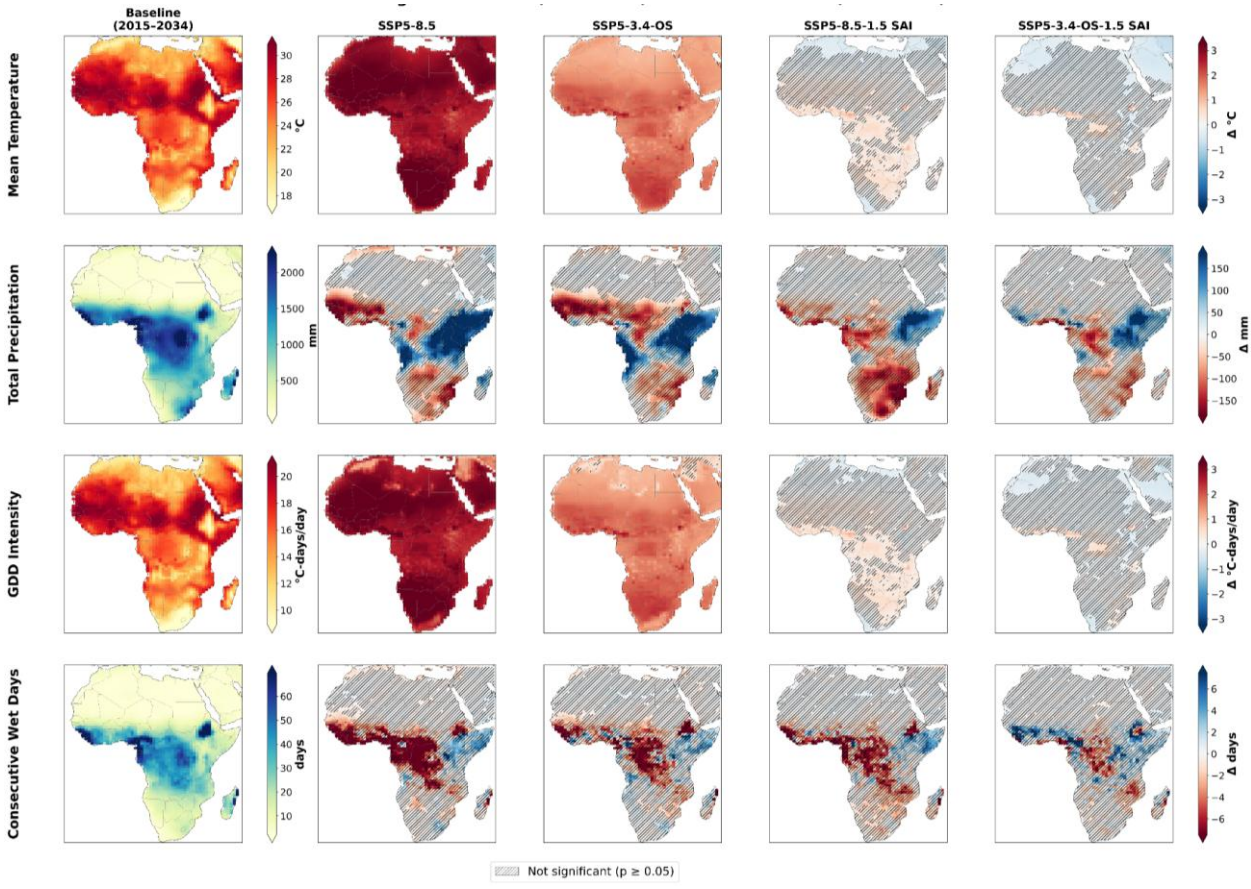

Figure 3: Spatial patterns of climate index changes during overshoot (2060 to 2079) relative to baseline (2015 to 2034). Rows: Mean Temperature, Total Precipitation, GDD Intensity, and Consecutive Wet Days. Columns from left to right: baseline climatology, SSP5-8.5 minus baseline, SSP5-3.4-OS minus baseline, SSP5-8.5-1.5 SAI minus baseline, and SSP5-3.4-OS-1.5 SAI minus baseline. Hatching indicates regions where changes are not statistically significant ($p \geq 0.05$, Welch's t-test).

The spatial distribution of overshoot-period (2060 to 2079) changes relative to the 2015 to 2034 reference period reveals widespread and statistically significant temperature increases under both SSP5-8.5 and SSP5-3.4-OS (Fig. 3). Under SSP5-8.5, mean temperature increases are pervasive across the continent, with the largest warming concentrated in the Sahara and Sahel regions. Annual Growing Degree Days, which refer to an accumulated thermal unit above a base temperature of 10°C, representing heat accumulation for crop development (GDD), increase substantially, reflecting enhanced thermal accumulation that exceeds optimal thresholds for many tropical crops. GDD intensity follows a similar pattern, with statistically significant increases spanning nearly all African land areas. Warm spell duration shows the most dramatic response among the temperature indices, with the Warm Spell Duration Index (WSDI) increasing by over 200 days in

https://doi.org/10.5194/egusphere-2026-3436
Preprint. Discussion started: 30 June 2026

tropical regions under SSP5-8.5, meaning warm spell conditions occupy more than half the year in these areas. Optimal growing days decline across much of tropical Africa, particularly in equatorial West and Central Africa, where baseline temperatures already approach upper crop tolerance thresholds.

The SSP5-3.4-OS overshoot scenario produces qualitatively similar spatial patterns of temperature change but with reduced magnitude compared to SSP5-8.5, reflecting the lower radiative forcing at the end of the century despite the transient overshoot (Fig. 3). Mean temperature and annual GDD show statistically significant changes across 100% of the African land area under both SSP5-8.5 and SSP5-3.4-OS, while GDD intensity is significant over 99.9% and 97.5% of the area, respectively (Figure 3). The Warm Spell Duration Index similarly shows near-universal significance (100% and 99.7%). These results demonstrate that even under a limited overshoot pathway, temperature-related indices undergo significant changes over the continent by the end of the century and under a strong decarbonization effort.

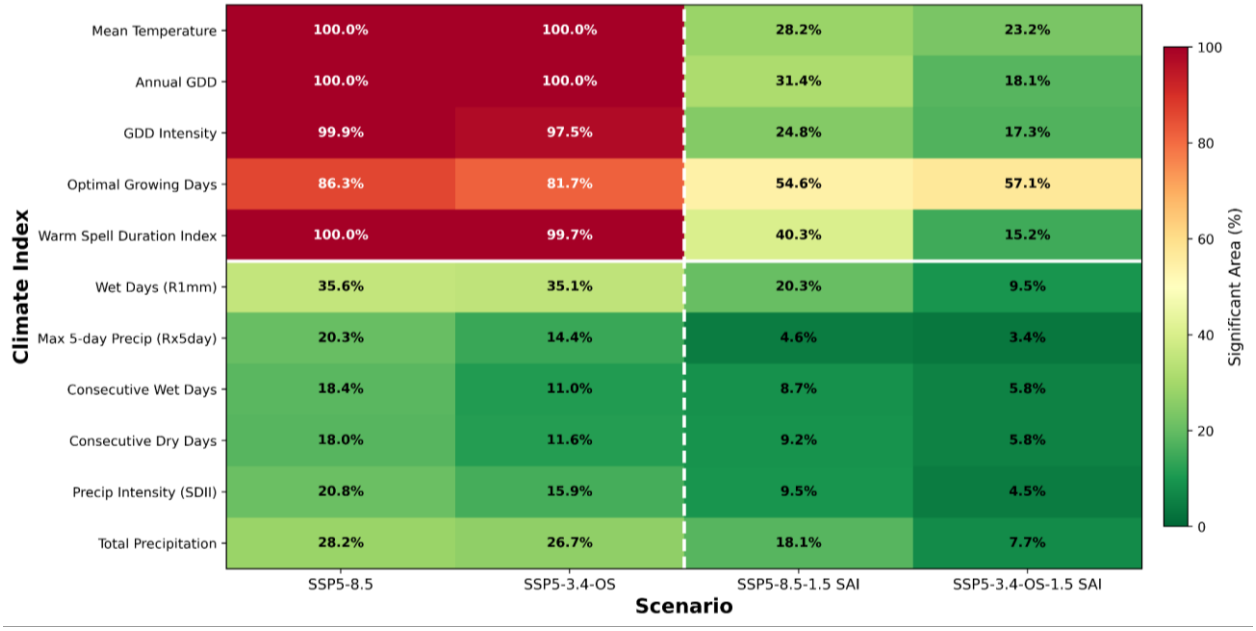

Figure 4: Detectability of climatic changes over land compared to a 1.5°C threshold. Heatmap showing the percentage of African land area with statistically significant changes ($p < 0.05$, Welch's t-test) in climate indices during the overshoot period (2060 to 2079). Columns represent scenarios (SSP5-8.5, SSP5-3.4-OS, SSP5-8.5-1.5 SAI, SSP5-3.4-OS-1.5 SAI); rows show indices grouped by temperature (top) and precipitation (bottom) categories. High values (red) indicate detectable changes over most of the continent; low values (green) indicate less widespread detectability.

Precipitation indices exhibit markedly more heterogeneous spatial patterns and lower statistical significance compared to temperature (Fig. 3). Significant changes in total precipitation cover 28.2% and 26.7% of the African land area under SSP5-8.5 and SSP5-3.4-OS, respectively, with wet days (R1mm) reaching 35.6% and 35.1%, and precipitation intensity (SDII) reaching 20.8% and 15.9% (Fig. 4). Consecutive wet and dry days show even lower coverage (18.4% and 18.0% under

https://doi.org/10.5194/egusphere-2026-3436
Preprint. Discussion started: 30 June 2026

SSP5-8.5; 11.0% and 11.6% under SSP5-3.4-OS), as does maximum 5-day precipitation (Rx5day) at 20.3% and 14.4% respectively. The spatial maps reveal a complex mosaic of wetting and drying: the Sahel and parts of East Africa show increase in total precipitation and in the number of wet days, while parts of Southern and Central Africa exhibit decreases (Fig 3). Maximum 5-day precipitation (Rx5day) shows increases concentrated over the Sahel and Horn of Africa under SSP5-8.5, indicating a tendency toward more intense precipitation events in these already vulnerable regions.

3.2 SAI effects on temperature and precipitation indices

SAI interventions consistently reduce all temperature indices across Africa relative to the SSP5-8.5 and SSP5-3.4-OS baselines during the overshoot period (Fig. 3). The cooling effect is spatially coherent, with the strongest reductions in tropical regions where baseline warming, the SSP5-8.5 scenario, is most pronounced. Under SSP5-8.5-1.5 SAI and SSP5-3.4-OS-1.5 SAI target scenarios, the percentage of land area showing statistically significant temperature changes drops substantially when SAI is applied. For mean temperature, significance declines from 100% under the baseline scenarios to 28.2% under SSP5-8.5-1.5 SAI and 23.2% under SSP5-3.4-OS-1.5 SAI (Fig. 4). The Warm Spell Duration Index shows an even more pronounced reduction, falling from 100% significance to 40.3% and 15.2% under the respective SAI scenarios. These reductions in statistical significance indicate that SAI effectively returns temperature conditions closer to the baseline state, narrowing the detectable departure from reference period climatology.

Precipitation responses to SAI display considerable spatial heterogeneity compared to the more uniform temperature cooling (Fig. 3). Parts of the Sahel show increased moisture availability under SAI relative to the high warming baselines, with localised increases in wet days and total precipitation. Central Africa exhibits mixed responses, with regional drying in parts of the Congo Basin alongside localised increases. East Africa demonstrates a dipole pattern characterised by coastal and highland wetting contrasted with interior drying, a pattern that intensifies under the higher 2.0°C warming threshold. The percentage of land area showing significant precipitation changes under SAI scenarios is generally comparable to or lower than under the baseline emission scenarios, with total precipitation significance at 18.1% under SSP5-8.5-1.5 SAI and 7.7% under SSP5-3.4-OS-1.5 SAI (Fig 4). This sensitivity to the magnitude of cooling arises because SAI alters precipitation through several pathways: stratospheric heating from sulfate aerosols shifts tropical rainfall patterns, and the reduction of shortwave radiation at the surface suppresses evaporation more strongly than it suppresses precipitation (Niemeier et al., 2013; Simpson et al., 2019; Tilmes et al., 2020; Visioni et al., 2021).

The surface moisture budget, defined as precipitation minus evapotranspiration (P minus E), reveals distinct regional trajectories across African monsoonal regions (Fig. 5).

https://doi.org/10.5194/egusphere-2026-3436
Preprint. Discussion started: 30 June 2026

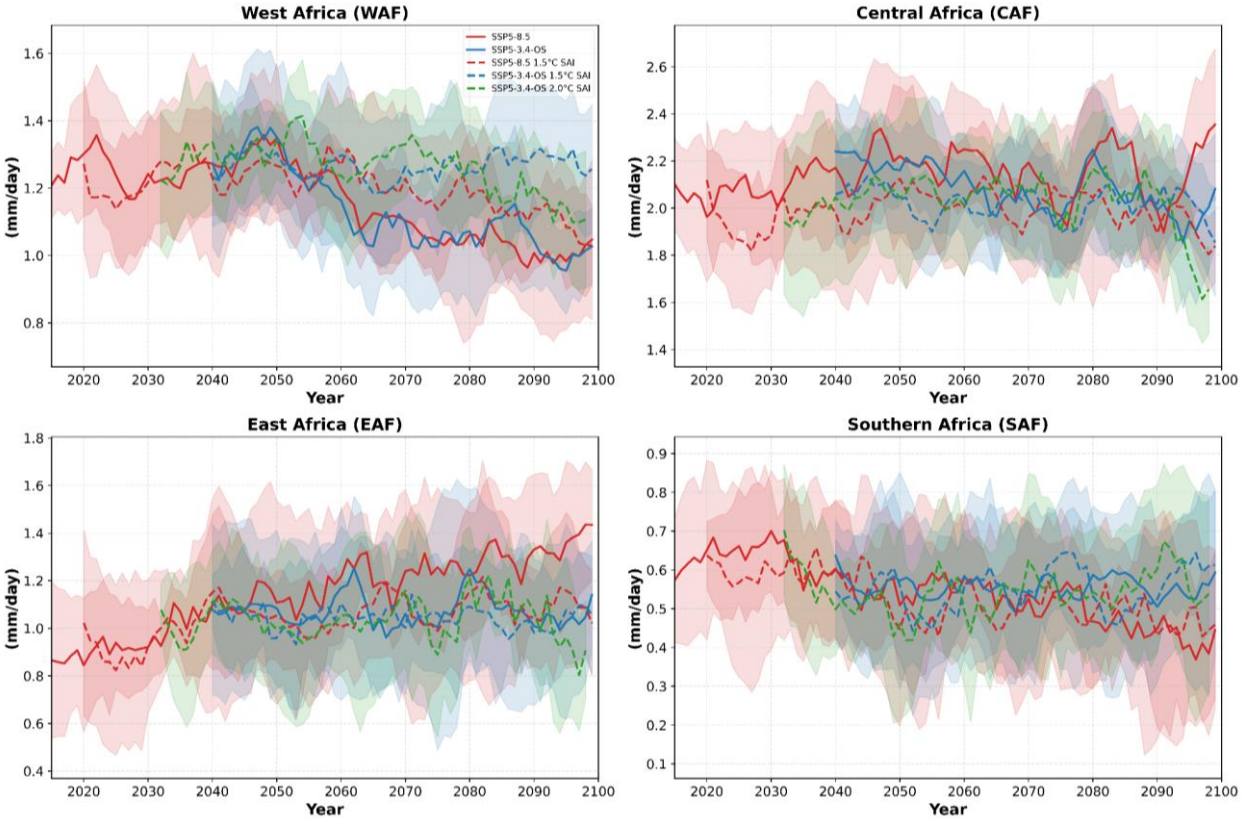

Figure 5: Surface moisture budget time series (P minus E) averaged over African monsoonal regions (2015 to 2099). Regional panels are shown for West Africa (WAF), Central Africa (CAF), East Africa (EAF) and Southern Africa (SAF). Lines represent 5-year running means; shading denotes ±1 standard deviation across ensemble members. Baseline scenarios (SSP5-8.5, SSP5-3.4-OS) and SAI scenarios targeting 1.5°C and 2.0°C are compared.

In West Africa (WAF), moisture availability declines progressively under SSP5-8.5 from approximately 1.3 mm/day to approximately 1.0 mm/day by 2100, representing a reduction of roughly 0.3 mm/day over the century. SAI scenarios maintain higher moisture levels, with values of approximately 1.2 to 1.3 mm/day sustained through 2100 under the 1.5°C and 2.0°C targets. This result indicates that SAI could help preserve surface water availability in West Africa during and beyond the overshoot period. Central Africa (CAF) exhibits relatively stable moisture conditions (approximately 2.0 to 2.2 mm/day) across all scenarios, though SAI produces slightly lower values than SSP5-8.5 toward the end of the century. East Africa (EAF) shows increasing moisture trends across all scenarios, with SSP5-8.5 producing the highest values and SAI scenarios yielding lower moisture levels than the high-warming baselines. Seasonal decomposition during the overshoot period (2060 - 2079) reveals that West Africa's moisture budget peaks during the JJA monsoon season (approximately 4 to 4.5 mm/day), while Central Africa maintains relatively high moisture throughout the year with peaks during the MAM and SON transitional seasons (Fig. 6). East Africa displays bimodal seasonality with maxima during MAM and SON,

https://doi.org/10.5194/egusphere-2026-3436
Preprint. Discussion started: 30 June 2026

corresponding to the long and short rainy seasons. Over Southern Africa, a decrease is projected during JJA and SON but peaks/increases during the DJF season. SAI scenarios generally result in reduced moisture availability relative to the high-warming baselines across all seasons and regions, though the magnitude varies by region.

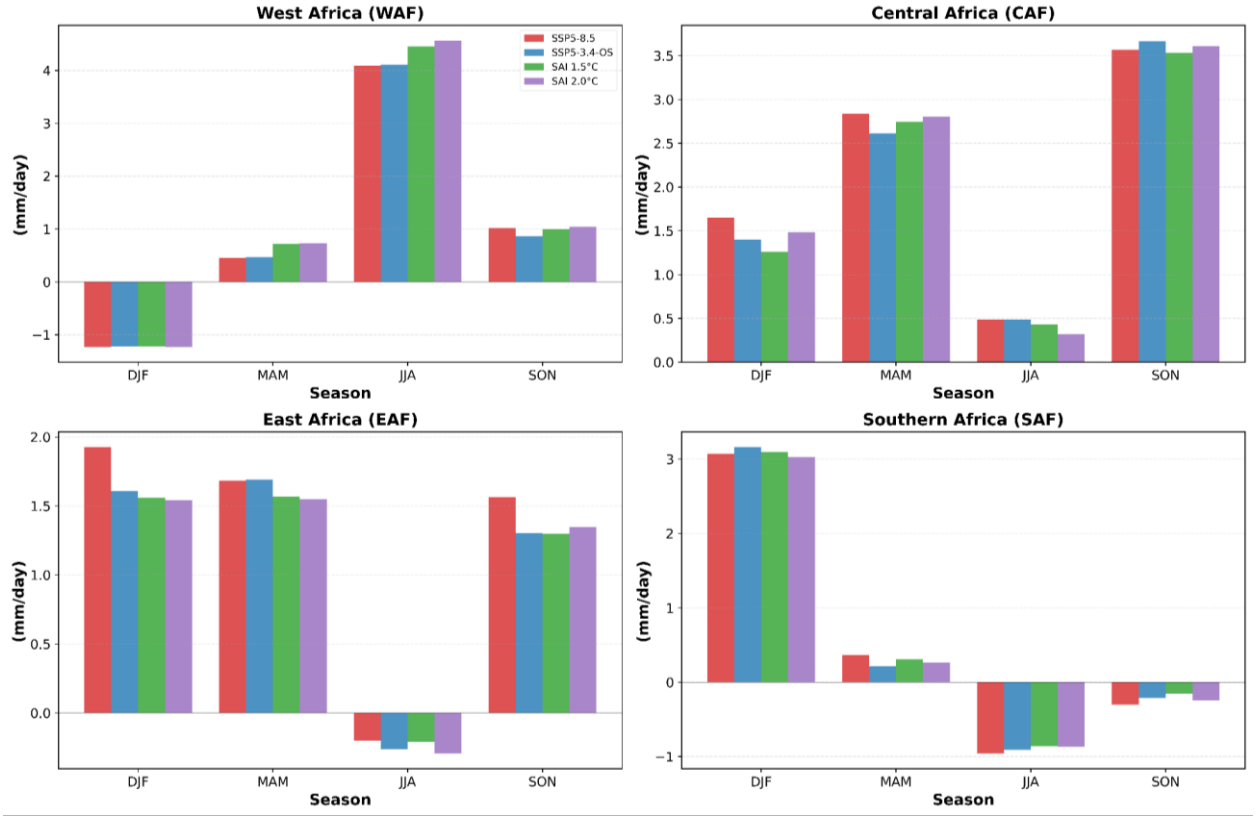

Figure 6: Seasonal surface moisture budget (P minus E) over African monsoonal regions during the overshoot period (2060 to 2079). Bar plots compare ensemble mean values across four scenarios (SSP5-8.5, SSP5-3.4-OS, SSP5-3.4-OS + SAI 1.5°C, SSP5-3.4-OS + SAI 2.0°C) for West Africa (WAF), Central Africa (CAF), East Africa (EAF) and Southern Africa (SAF) during DJF, MAM, JJA, and SON seasons.

The surface moisture budget, defined as precipitation minus evapotranspiration (P minus E), reveals distinct regional trajectories across African monsoonal regions (Fig. 4). In West Africa (WAF), moisture availability declines progressively under SSP5-8.5 from approximately 1.3 mm/day to approximately 1.0 mm/day by 2100, representing a reduction of roughly 0.3 mm/day over the century. SAI scenarios maintain higher moisture levels, with values of approximately 1.2 to 1.3 mm/day sustained through 2100 under the 1.5°C and 2.0°C targets. This result indicates that SAI could help preserve surface water availability in West Africa during and beyond the overshoot period. Central Africa (CAF) exhibits relatively stable moisture conditions (approximately 2.0 to 2.2 mm/day) across all scenarios, though SAI produces slightly lower values than SSP5-8.5 toward the end of the century. East Africa (EAF) shows increasing moisture trends across all scenarios, with SSP5-

https://doi.org/10.5194/egusphere-2026-3436
Preprint. Discussion started: 30 June 2026

8.5 producing the highest values and SAI scenarios yielding lower moisture levels than the high-warming baselines. Seasonal decomposition during the overshoot period (2060 - 2079) reveals that West Africa's moisture budget peaks during the JJA monsoon season (approximately 4 to 4.5 mm/day), while Central Africa maintains relatively high moisture throughout the year with peaks during the MAM and SON transitional seasons (Fig. 6). East Africa displays bimodal seasonality with maxima during MAM and SON, corresponding to the long and short rainy seasons. Over Southern Africa, a decrease is projected during JJA and SON but peaks/increases during the DJF season. SAI scenarios generally result in reduced moisture availability relative to the high-warming baselines across all seasons and regions, though the magnitude varies by region.

The spatial distribution of the surface moisture budget reveals contrasting regional responses across Africa during the overshoot period (Fig. 7). East Africa emerges as the greatest beneficiary, with increases of approximately 0.5 mm/day, while Southern Africa experiences the largest reduction at approximately 0.3 mm/day. Central Africa shows a mixed response, with moistening in the south-west and drying in the north-west of the region, and West Africa shows a moderate increase of approximately 0.4 mm/day. The spatial distribution shows a similar pattern to the variability and seasonal surface moisture budget in Figs. 5 and 6, respectively. The variation in surface moisture budget may lead to a regional impact on precipitation due to the overshoot scenario, as shown in Tilmes et al. (2020). The study further revealed a reduction in precipitation in the southern hemisphere, which further supports our findings of the reduction in the surface moisture budget in southern Africa between the 2060-2079 period in our study (Tilmes et al., 2020).

https://doi.org/10.5194/egusphere-2026-3436
Preprint. Discussion started: 30 June 2026

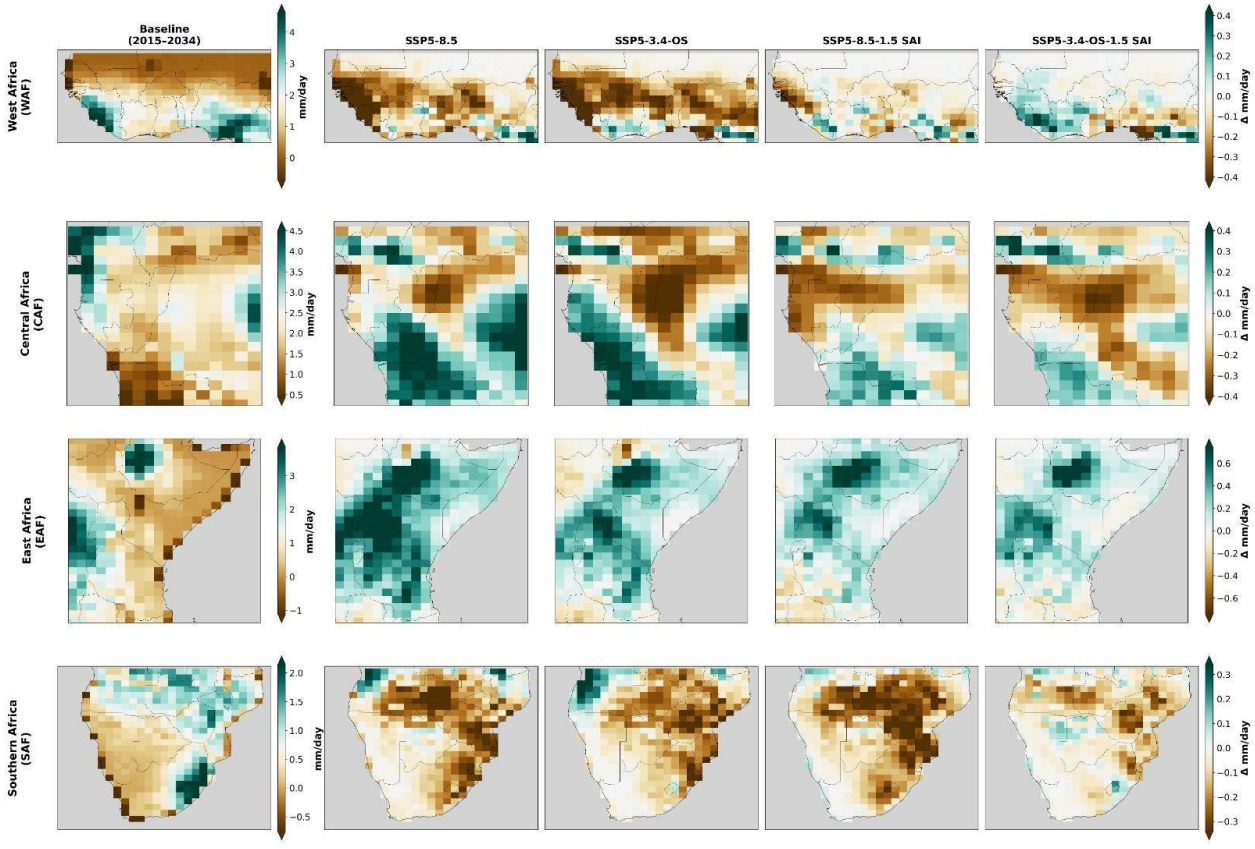

Figure 7: Spatial patterns of SAI effects on surface moisture budget during the overshoot period (2060-2079). Each panel shows the difference between the SAI scenario and the corresponding baseline (SAI minus baseline). Columns compare SAI at 1.5°C and 2.0°C targets against SSP5-8.5 and SSP5-3.4-OS baselines. West Africa shows predominantly increased moisture availability under SAI, particularly in the Sahel. Central Africa exhibits mixed responses with regional drying in parts of the Congo Basin. East Africa displays contrasting patterns with coastal increases and interior decreases, while regional drying is exhibited in southern Africa. The magnitude of moisture changes varies with both the SAI target temperature and baseline scenario.

4. Discussion and Conclusion

The results of this study provide important information on how temperature overshoot and SAI affect the African climate. Our findings show temperature responses are spatially coherent and highly detectable, while precipitation and moisture responses are regionally differentiated and less statistically robust. This asymmetry has important implications for understanding the potential impacts of overshoot pathways and the potential benefits and risks of climate intervention strategies for the African continent.

https://doi.org/10.5194/egusphere-2026-3436
Preprint. Discussion started: 30 June 2026

The near-universal significance of temperature index changes (ranging from 86% to 100% of African land area for most metrics, as shown in Fig. 4 during the overshoot period confirms that transient warming produces continent-wide thermal stress regardless of the emission pathway. The Warm Spell Duration Index is particularly instructive: under SSP5-8.5, warm spells effectively become quasi-permanent features of the tropical African climate, a finding consistent with Glade et al. (2025), who reported similar shifts in warm spell characteristics under SSP2-4.5 using the same CESM2-WACCM6 framework. The magnitude of GDD increases, and optimal growing day reductions point to direct consequences for crop phenology and yield, as thermal accumulation increasingly exceeds the tolerance ranges of major staple crops (Challinor et al., 2014). That the SSP5-3.4-OS pathway, despite its eventual decline in radiative forcing, produces temperature responses of comparable significance to SSP5-8.5 during the overshoot window underscores a critical finding: the transient overshoot period itself, not just the end-of-century state, poses substantial risks to African agricultural systems.

SAI proves highly effective at moderating these temperature extremes, reducing the statistical significance of temperature changes from near-universal levels to between 15% and 57%, depending on the index and scenario. This capacity to reduce peak warming is consistent with the design intent of the feedback-controlled injection strategy employed in the CESM2-WACCM6 experiments (Tilmes et al., 2020), which adjusts SO_2 injection rates at four stratospheric locations (15°N, 15°S, 30°N, and 30°S) to maintain global mean temperatures near the target threshold. This four-point configuration gives the feedback algorithm enough degrees of freedom to maintain not only the global mean temperature but also the interhemispheric and equator-to-pole temperature gradients, avoiding the disproportionate tropical cooling that single-point equatorial injection would produce (Kravitz et al., 2017; Richter et al., 2022). From an agricultural perspective, the proposed SAI cooling is potentially advantageous, as it coincides with the regions where baseline temperatures are already closest to or exceeding crop thermal limits.

The precipitation responses are considerably more complex. The heterogeneous spatial patterns of precipitation change, with only 11% to 36% of land area showing statistical significance for most indices, reflect the well-documented challenge of detecting forced precipitation signals amid large internal variability in tropical precipitation (Hawkins and Sutton, 2011). Nevertheless, the spatial patterns that emerge are physically consistent with known mechanisms. The localised increases in Sahelian precipitation under SAI projected in our results align broadly with Pinto et al. (2020), who found that SAI partially offsets projected precipitation changes in parts of the Sahel. However, Da-Allada et al. (2020) demonstrated that SAI designed to offset all warming would be over effective in Western Africa, reversing a modest positive precipitation trend into a negative one through weakened monsoon circulation driven by reduced low-level land-sea thermal contrast. This subregional complexity within West Africa is consistent with the mixed precipitation signals, seen here. The East African dipole of coastal wetting and interior drying reflects the complex interplay between Indian Ocean moisture transport and continental convective dynamics, patterns identified in observational analyses of the region's rainfall variability (Nicholson, 2017).

https://doi.org/10.5194/egusphere-2026-3436
Preprint. Discussion started: 30 June 2026

The surface moisture budget analysis provides a crucial agronomic dimension beyond what individual precipitation indices can capture (Fig. 7). The progressive drying of West Africa under SSP5-8.5 (approximately 0.3 mm/day decline by 2100) reflects not only precipitation changes but also the enhanced evaporative demand associated with rising temperatures. SAI's ability to maintain higher moisture levels in West Africa derives from its partial restoration of precipitation and its reduction of temperature-driven evapotranspiration, a dual mechanism that highlights the importance of considering the full surface water balance rather than precipitation alone. In Central Africa, the relative stability of moisture conditions across scenarios likely reflects the buffering role of the Congo Basin's extensive forest cover and recycled moisture (Pokam et al., 2012). The higher moisture levels under SSP5-8.5 compared to SAI in East Africa can be explained by the thermodynamic increase in atmospheric moisture capacity under warming, which delivers greater precipitation totals to the region's orographic lifting zones despite the concurrent increase in evaporative demand.

Crucially, our findings demonstrate that some potential impacts of SAI are scenario-dependent: excessive drying in some regions is a function of large amounts of SAI-driven cooling but can be mitigated if the underlying emission scenario is lower. This points to the necessity of considering SAI not as a replacement, but as a complement to strong decarbonization efforts through mitigation and CDR, so that temperatures (which would increase even under an overshoot) can be kept low while modifications to the hydrological cycle can be minimized, thereby potentially minimizing crop vulnerability.

Several caveats should be noted when interpreting these findings. First, the analysis relies on a single Earth system model (CESM2-WACCM6), and precipitation responses to greenhouse gas forcing and SAI are known to differ substantially across models (Visioni et al., 2021; Nkrumah et al., 2025; Kumi et al., 2025). Multi-model assessments are necessary to establish the robustness of the regional precipitation patterns identified here. Second, the statistical testing framework based on Welch's t-test applied to ensemble members may have limited power for detecting changes in indices with high spatial and temporal variability, potentially underestimating the true extent of significant precipitation changes. Third, this study treats the surface moisture budget as P minus E averaged over broad subregions, which may obscure important sub-regional gradients, particularly in East Africa, where topographic complexity creates sharp moisture contrasts over short distances, highlighting the need for higher resolution ensembles also including SAI strategies.

Despite these limitations, the findings carry direct implications for climate adaptation planning in Africa. The asymmetry between highly detectable temperature changes and less detectable but regionally important precipitation changes suggests that agricultural planning should prioritize heat stress adaptation as a robust response to overshoot risk, while precipitation-related decisions will require more regionally tailored strategies. The demonstrated effectiveness of SAI at moderating temperature extremes across the continent, combined with its capacity to preserve surface moisture in West Africa, indicates that climate intervention under a limited overshoot could substantially reduce thermal hazards for African agriculture. However, the spatial heterogeneity of precipitation responses, including the potential for drying in parts of the Congo Basin

https://doi.org/10.5194/egusphere-2026-3436
Preprint. Discussion started: 30 June 2026

and interior East Africa, reinforces the need for careful, region-specific impact assessment before any consideration of SAI deployment.

Furthermore, these results suggest SAI may be more effective when combined with aggressive mitigation under the overshoot pathway than under sustained high emissions. As shown in Tilmes et al. (2020), the SSP5-3.4-OS scenario requires lower annual SO_2 injection rates compared to the SSP5-8.5 baseline, as the lower background greenhouse gas forcing reduces the radiative offset needed to maintain target temperatures. This reduced injection translates to smaller hydrological perturbations, as evidenced by the lower precipitation significance values under SSP5-3.4-OS-1.5 SAI across nearly all indices (Fig. 4). These results support the framing of SAI as a temporary peak-shaving measure alongside aggressive mitigation, rather than as a substitute for emission reductions.

In summary, temperature overshoot produces near-universal, statistically significant changes in temperature-related agroclimatic indices across Africa, whereas precipitation indices show more heterogeneous and less detectable responses. SAI effectively moderates temperature extremes across Africa, with the strongest benefits in tropical Africa, but its precipitation and moisture effects vary by region, scenario, and season. The surface moisture budget analysis reveals that SAI would be most beneficial for West Africa, where it counteracts progressive drying, while Central Africa remains relatively insensitive, and East Africa's response involves trade-offs between reduced warming and altered moisture availability. These results underscore that the evaluation of climate intervention strategies for Africa must extend beyond global mean temperature targets to encompass the full spectrum of agroclimatic variables that determine agricultural viability and water security across the continent's diverse climate regions.

https://doi.org/10.5194/egusphere-2026-3436
Preprint. Discussion started: 30 June 2026

Appendix A

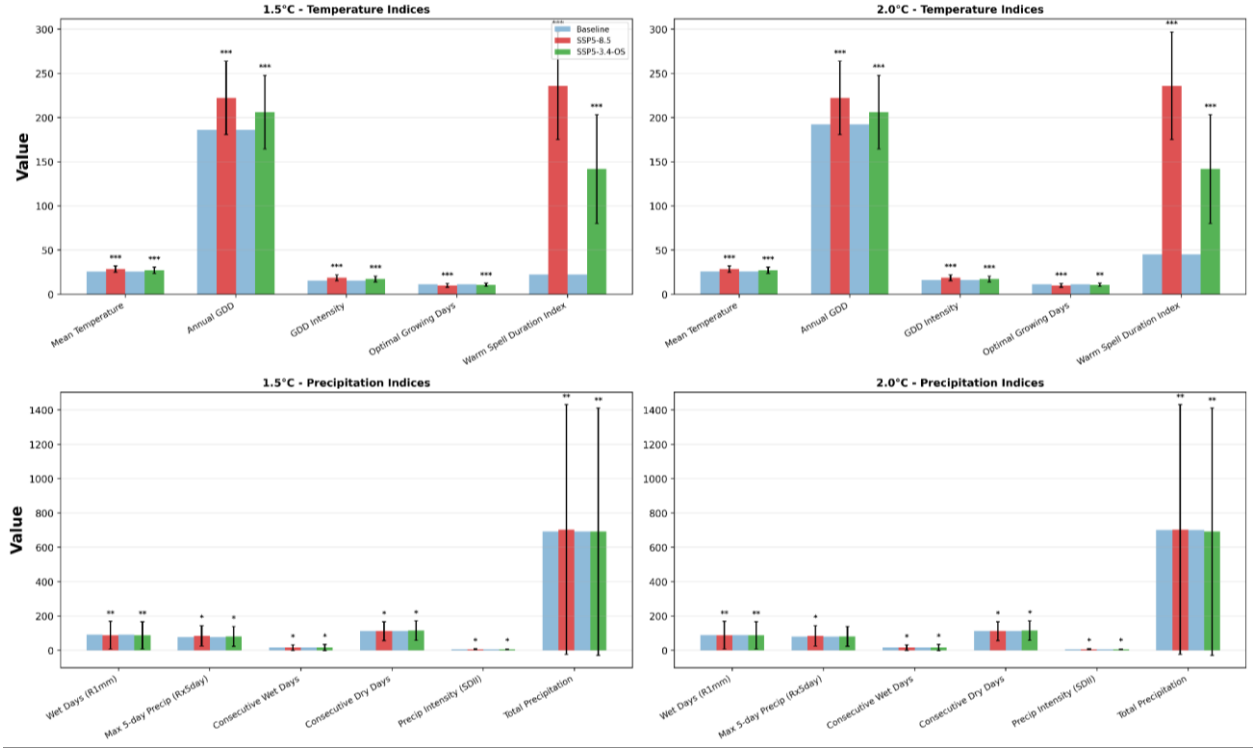

Figure A1. Baseline versus overshoot period comparison at combined thresholds (1.5°C and 2.0°C). Top panels: temperature indices (Mean Temperature, Annual GDD, GDD Intensity, Optimal Growing Days, Warm Spell Duration Index). Bottom panels: precipitation indices (Wet Days, Max 5-day Precip, Consecutive Wet Days, Consecutive Dry Days, Precipitation Intensity, Total Precipitation). Asterisks denote statistical significance (*: >10%, **: >25%, ***: >50% significant area). Error bars show ±1 standard deviation.

https://doi.org/10.5194/egusphere-2026-3436
Preprint. Discussion started: 30 June 2026

Appendix B

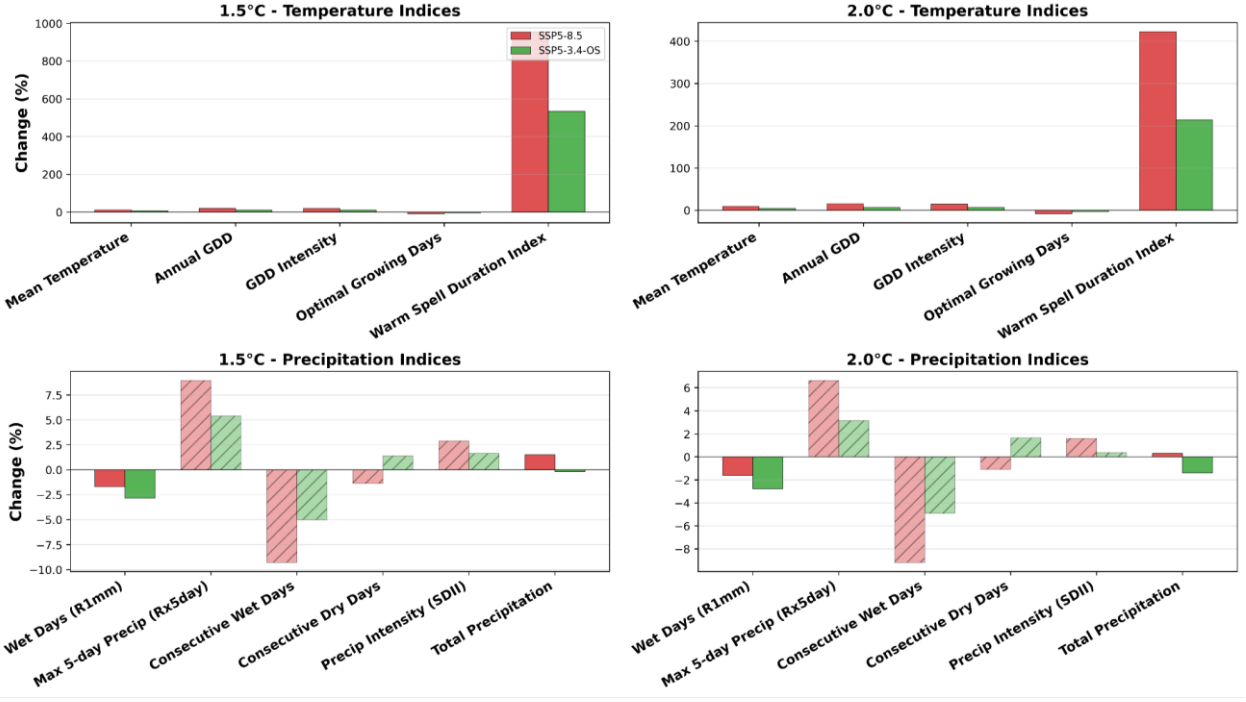

Figure A2: Percentage change in climate indices from baseline to overshoot period (2060-2079) for 1.5°C and 2.0°C thresholds. Error bars indicate propagated uncertainty from spatial variability. Temperature-related indices show 5-30% increases depending on the metric, while precipitation indices range from -10% to +15% with greater uncertainty.

https://doi.org/10.5194/egusphere-2026-3436
Preprint. Discussion started: 30 June 2026

480

Appendix C

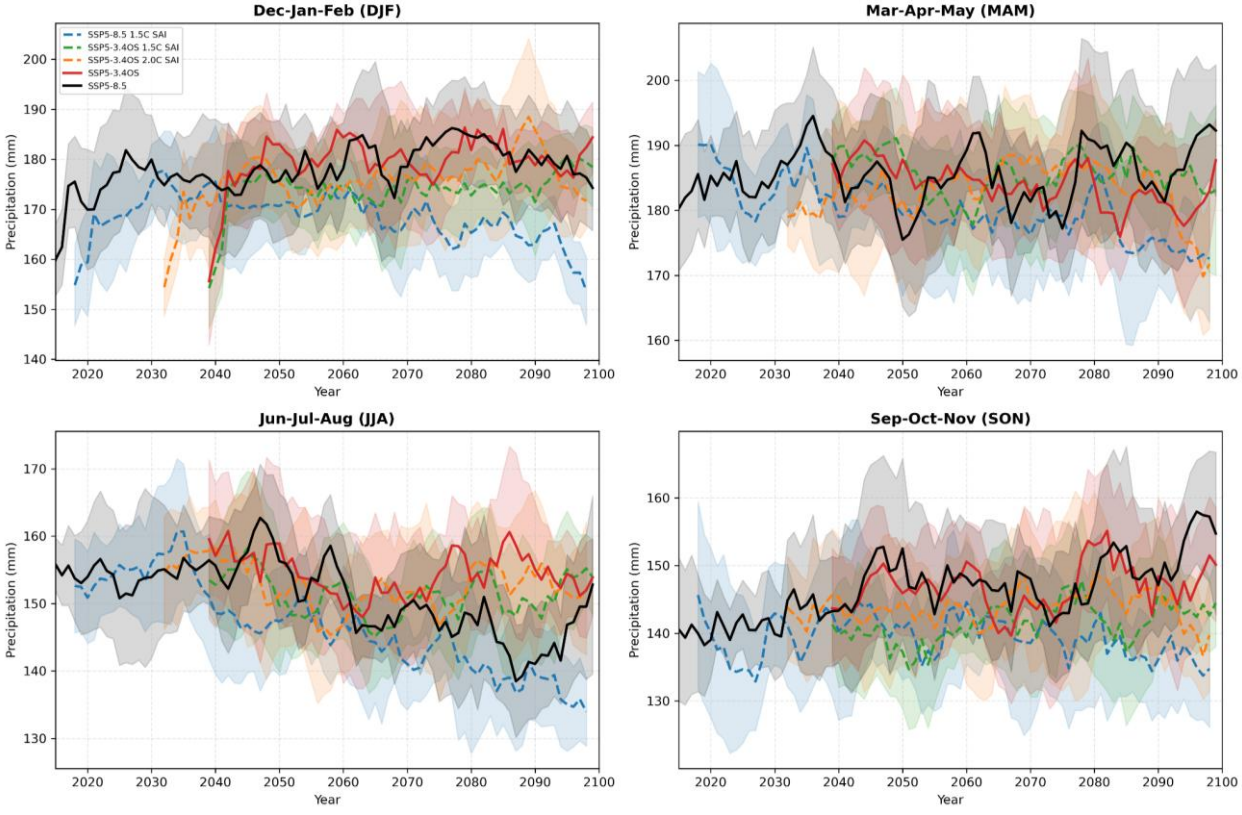

Figure A3: Seasonal precipitation (2015-2099) over Africa. Lines: 5-year running mean; shading: ±1 standard deviation across ensemble members

485

490

https://doi.org/10.5194/egusphere-2026-3436
Preprint. Discussion started: 30 June 2026

Code and data availability

The CESM2 WACCM6 SSP5-85 and SSP5-34-OS data analyzed in this paper have been contributed to CMIP6 and are freely available at the Earth System Grid Federation (ESGF; https://esgf-node.llnl.gov/search/cmip6/) (ESGF, 2020) or from the NCAR Digital Asset Services Hub (DASH; https://data.ucar.edu) (NCAR, 2020b) or from the links provided from the CESM website (http://www.cesm.ucar.edu/) (NCAR, 2020c) as well as in (Danabasoglu, 2020). The analysis code used to compute climate indices, the surface moisture budget, and the detectability heatmap is openly available on GitHub at https://github.com/Temmywork/sai-overshoot-analysis and archived on Zenodo at https://doi.org/10.5281/zenodo.20342083 .

Author contributions

TSE: Conceptualisation, Formal analysis, Methodology, Visualisation, Writing – original draft; **TSF:** Conceptualisation, Formal analysis, Methodology, Visualisation, Writing – original draft, review & editing; **DV:** Conceptualisation, Methodology, Writing – review & editing; **RCO:** Conceptualisation, Writing – review & editing; **ABJ:** Methodology, Writing – review & editing; **ST:** Model Experiment, Writing – review & editing; **CL:** Writing – review & editing; **MGN:** Conceptualisation, Writing – review & editing

Competing interests

The authors declare that the research was conducted in the absence of any commercial or financial relationships that could be construed as a potential conflict of interest.

Acknowledgements

The authors acknowledge the NSF National Centre for Atmospheric Research, a major facility sponsored by the National Science Foundation under Cooperative Agreement No. 1755088 for their efforts in producing the experiments used in the present study and for making them publicly available.

Financial support

This study was supported by Simons Foundation Grant. The first author is also supported by GRID-CC project through the ARIA fund, UK. The funder played no role in study design, data collection, analysis and interpretation of data, or the writing of this manuscript.

https://doi.org/10.5194/egusphere-2026-3436
Preprint. Discussion started: 30 June 2026

References

Almazroui, M., Saeed, F., Saeed, S., Islam, M. N., Ismail, M., Klutse, N. A. B., & Siddiqui, M. H. (2020). Projected change in temperature and precipitation over Africa from CMIP6. Earth Systems and Environment, 4, 455–475. https://doi.org/10.1007/s41748-020-00161-x

Arias, P. A., Bellouin, N., Coppola, E., Jones, R. G., Krinner, G., Marotzke, J., et al. (2021). Technical Summary. In V. Masson-Delmotte, P. Zhai, A. Pirani, S. L. Connors, C. Péan, S. Berger, N. Caud, Y. Chen, L. Goldfarb, M. I. Gomis, M. Huang, K. Leitzell, E. Lonnoy, J. B. R. Matthews, T. K. Maycock, T. Waterfield, O. Yelekçi, R. Yu, & B. Zhou (Eds.), Climate Change 2021: The Physical Science Basis. Contribution of Working Group I to the Sixth Assessment Report of the Intergovernmental Panel on Climate Change (pp. 33–144). Cambridge University Press. https://doi.org/10.1017/9781009157896.002

Boucher, O., Halloran, P. R., Burke, E. J., Doutriaux-Boucher, M., Jones, C. D., Lowe, J., ... & Wu, P. (2012). Reversibility in an Earth System model in response to CO_2 concentration changes. Environmental Research Letters, 7(2), 024013. https://doi.org/10.1088/1748-9326/7/2/024013

Bourgault, P., Huard, D., Smith, T. J., Logan, T., Aoun, A., Lavoie, J., et al. (2023). xclim: xarray-based climate data analytics. Journal of Open Source Software, 8(85), 5415. https://doi.org/10.21105/joss.05415

Challinor, A. J., Watson, J., Lobell, D. B., Howden, S. M., Smith, D. R., and Chhetri, N. (2014). A meta-analysis of crop yield under climate change and adaptation. Nature Climate Change, 4(4), 287–291. https://doi.org/10.1038/nclimate2153

Cook, K. H. (1999). Generation of the African easterly jet and its role in determining West African precipitation. Journal of Climate, 12(5), 1165–1184. https://doi.org/10.1175/1520-0442(1999)012<1165:GOTAEJ>2.0.CO;2

Da-Allada, C. Y., Baloitcha, E., Alamou, E. A., Awo, F. M., Bonou, F., Pomalegni, Y., Biao, E. I., Obada, E., Zandagba, J. E. B., Tilmes, S., and Irvine, P. J. (2020). Changes in West African summer monsoon precipitation under stratospheric aerosol geoengineering. Earth's Future, 8(7), e2020EF001595. https://doi.org/10.1029/2020EF001595

Danabasoglu, G., Lamarque, J.-F., Bacmeister, J., Bailey, D. A., DuVivier, A. K., Edwards, J., et al. (2020). The Community Earth System Model Version 2 (CESM2). Journal of Advances in Modeling Earth Systems, 12(2), e2019MS001916. https://doi.org/10.1029/2019MS001916

https://doi.org/10.5194/egusphere-2026-3436
Preprint. Discussion started: 30 June 2026

Egbebiyi, T. S., Ajayi, V. O., Arowolo, A. V., Ogunniyi, J., & Ogunjo, S. (2025a). The effect of solar radiation modification on agroclimatic indices in Africa. *Environ. Res.: Climate 4 (2025) 035003*. https://doi.org/10.1088/2752-5295/ade619

Emmons, L. K., Schwantes, R. H., Orlando, J. J., Tyndall, G., Kinnison, D., Lamarque, J.-F., et al. (2020). The Chemistry Mechanism in the Community Earth System Model Version 2 (CESM2). Journal of Advances in Modeling Earth Systems, 12(4), e2019MS001882. https://doi.org/10.1029/2019MS001882

Eyring, V., Bony, S., Meehl, G. A., Senior, C. A., Stevens, B., Stouffer, R. J., & Taylor, K. E. (2016). Overview of the Coupled Model Intercomparison Project Phase 6 (CMIP6) experimental design and organization. Geoscientific Model Development, 9(5), 1937–1958. https://doi.org/10.5194/gmd-9-1937-2016

Glade, R. C., Tye, M. R., Visioni, D., Kravitz, B., and Richter, J. H. (2025). SAI deployment reduces warm spell occurrence, duration, and intensity. Frontiers in Climate, 7, 1581305. https://doi.org/10.3389/fclim.2025.1581305

Gettelman, A., Mills, M. J., Kinnison, D. E., Garcia, R. R., Smith, A. K., Marsh, D. R., et al. (2019). The Whole Atmosphere Community Climate Model Version 6 (WACCM6). Journal of Geophysical Research: Atmospheres, 124(23), 12380–12403. https://doi.org/10.1029/2019JD030943

Hawkins, E. and Sutton, R. (2011). The potential to narrow uncertainty in projections of regional precipitation change. Climate Dynamics, 37(1–2), 407–418. https://doi.org/10.1007/s00382-010-0810-6

Iturbide, M., Gutiérrez, J. M., Alves, L. M., Bedia, J., Cerezo-Mota, R., Cimadevilla, E., et al. (2020). An update of IPCC climate reference regions for subcontinental analysis of climate model data: definition and aggregated datasets. Earth System Science Data, 12(4), 2959–2970. https://doi.org/10.5194/essd-12-2959-2020

Kravitz, B., MacMartin, D. G., Mills, M. J., Richter, J. H., Tilmes, S., Lamarque, J., Tribbia, J.J., and Vitt, F. (2017). First simulations of designing stratospheric sulfate aerosol geoengineering to meet multiple simultaneous climate objectives J. Geophys. Res. Atmos. 122 12–616

Klutse, N. A. B., Ajayi, V. O., Gbobaniyi, E. O., Egbebiyi, T. S., Kouadio, K., Nkrumah, F., ... & Sylla, M. B. (2018). Potential impact of 1.5°C and 2°C global warming on consecutive dry and wet days over West Africa. Environmental Research Letters, 13(5), 055013. https://doi.org/10.1088/1748-9326/aab37b

Kumi, N., Mensah, C., Quagraine, K. A., Patel, T. D., Otu-Larbi, F., Prempeh, N. A., Nguvava, M., Nkemelang, T., Abiodun, B. J., Lennard, C., New, M. G., and Odoulami, R. C. (2025). Africa's regional and local climate response to stratospheric aerosol injection characteristics. Frontiers in Climate, 7, 1599405. https://doi.org/10.3389/fclim.2025.1599405

https://doi.org/10.5194/egusphere-2026-3436
Preprint. Discussion started: 30 June 2026

Liu, X., Ma, P.-L., Wang, H., Tilmes, S., Singh, B., Easter, R. C., Ghan, S. J., & Rasch, P. J. (2016). Description and evaluation of a new four-mode version of the Modal Aerosol Module (MAM4) within version 5.3 of the Community Atmosphere Model. Geoscientific Model Development, 9(2), 505–522. https://doi.org/10.5194/gmd-9-505-2016

MacMartin, D. G., Kravitz, B., Tilmes, S., Richter, J. H., Mills, M. J., Lamarque, J.-F., Tribbia, J. J., & Vitt, F. (2017). The climate response to stratospheric aerosol geoengineering can be tailored using multiple injection locations. Journal of Geophysical Research: Atmospheres, 122(23), 12574–12590. https://doi.org/10.1002/2017JD026868

MacMartin, D.G., Ricke, K.L., Keith, D.W., Mitchell, D., Allen, M.R., Hall, J.W., Mueller, B., Rajamani, L. and Quéré, C.L. (2018). Solar geoengineering as part of an overall strategy for meeting the 1.5 C Paris target. *Philosophical Transactions of the Royal Society A: Mathematical, Physical and Engineering Sciences*, *376*(2119) https://doi.org/10.1098/rsta.2016.0454

Mupangwa, W., Twomlow, S., & Walker, S. (2016). Reduced tillage and nitrogen effects on soil 895 water dynamics and maize (Zea mays L.) yield under semi-arid conditions. International Journal 896 of Agricultural Sustainability, 14(1), 13-30.

Nicholson, S. E. (2013). The West African Sahel: A review of recent studies on the rainfall regime and its interannual variability. ISRN Meteorology, 2013, 453521. https://doi.org/10.1155/2013/453521

Ofori, I. K., & Asongu, S. (2021). Foreign direct investment, governance and inclusive growth in 914 sub-Saharan Africa. Governance and Inclusive Growth in Sub-Saharan Africa (June 7, 2021)

O'Neill, B. C., Tebaldi, C., van Vuuren, D. P., Eyring, V., Friedlingstein, P., Hurtt, G., et al. (2016). The Scenario Model Intercomparison Project (ScenarioMIP) for CMIP6. Geoscientific Model Development, 9(9), 3461–3482. https://doi.org/10.5194/gmd-9-3461-2016

Nicholson, S. E. (2017). Climate and climatic variability of rainfall over eastern Africa. Reviews of Geophysics, 55(3), 590–635. https://doi.org/10.1002/2016RG000544

Nkrumah, F., Quagraine, K. A., Klutse, N. A. B., Quenum, G. M. L. D., Nkrumah, L. A., and Dommo, A. (2025). Assessing regional climate trends in West Africa under geoengineering: A multimodel comparison of UKESM1 and CESM2. Journal of Geophysical Research: Atmospheres, 130, e2024JD043117. https://doi.org/10.1029/2024JD043117

Patel, T. D., Odoulami, R. C., Pinto, I., Egbebiyi, T. S., Lennard, C., Abiodun, B. J., & New, M. (2023). Potential impact of stratospheric aerosol geoengineering on projected temperature and precipitation extremes in South Africa. Environmental Research: Climate, 2, 035004. https://doi.org/10.1088/2752-5295/acdaec

Peterson, T. C. (2005). Climate change indices. WMO Bulletin, 54(2), 83–86.

https://doi.org/10.5194/egusphere-2026-3436
Preprint. Discussion started: 30 June 2026

Pinto, I., Jack, C., Lennard, C., Tilmes, S., & Odoulami, R. C. (2020). Africa's climate response to solar radiation management with stratospheric aerosol. Geophysical Research Letters, 47, e2019GL086047. https://doi.org/10.1029/2019GL086047

Pokam, W. M., Djiotang, L. A. T., and Mkankam, F. K. (2012). Atmospheric water vapour transport and recycling in equatorial Central Africa through NCEP/NCAR reanalysis data. Climate Dynamics, 38(9–10), 1715–1729. https://doi.org/10.1007/s00382-011-1242-7

Quagraine, K. A., Tye, M. R., Quagraine, K. T., Tilmes, S., Simpson, I. R., Nkrumah, F., Egbebiyi, T. S., Odoulami, R. C., & Klutse, N. A. B. (2025). Assessing the impact of stratospheric aerosol injection on precipitation extremes in Africa using the ARISE-SAI-1.5 dataset. Environmental Research: Climate, 4, 035006. https://doi.org/10.1088/2752-5295/adee3c

Richter, J. H., Tilmes, S., Mills, M. J., Tribbia, J. J., Kravitz, B., MacMartin, D. G., Vitt, F., and Lamarque, J.-F. (2017). Stratospheric dynamical response and ozone feedbacks in the presence of SO2 injections. Journal of Geophysical Research: Atmospheres, 122, 12557–12573. https://doi.org/10.1002/jgrd.54286

Richter, J. H., Visioni, D., MacMartin, D. G., Bailey, D. A., Rosenbloom, N., Dobbins, B., Lee, W. R., Tye, M., & Lamarque, J. F. (2022). Assessing responses and impacts of solar climate intervention on the Earth system with stratospheric aerosol injection (ARISE-SAI): protocol and initial results from the first simulations. Geoscientific Model Development, 15, 8221–8243. https://doi.org/10.5194/gmd-15-8221-2022

Sultan, B., & Gaetani, M. (2016). Agriculture in West Africa in the twenty-first century: climate change and impacts scenarios, and potential for adaptation. Frontiers in Plant Science, 7, 1262. https://doi.org/10.3389/fpls.2016.01262

Sylla, M. B., Nikiema, P. M., Gibba, P., Kebe, I., & Klutse, N. A. B. (2016). Climate change over West Africa: recent trends and future projections. In: Adaptation to Climate Change and Variability in Rural West Africa (pp. 25–40). Springer. https://doi.org/10.1007/978-3-319-31499-0_3

Tebaldi, C., Debeire, K., Eyring, V., Fischer, E., Fyfe, J., Friedlingstein, P., ... & Sanderson, B. (2021). Climate model projections from the Scenario Model Intercomparison Project (ScenarioMIP) of CMIP6. Earth System Dynamics, 12, 253–293. https://doi.org/10.5194/esd-12-253-2021

Tilmes, S., Sanderson, B. M. & O'Neill, B. C. (2016). Climate impacts of geoengineering in a delayed mitigation scenario, Geophys. Res. Lett., 43, 8222–8229 https://doi.org/10.1002/2016GL070122

Tilmes, S., Richter, J. H., Kravitz, B., MacMartin, D. G., Mills, M. J., Simpson, I. R., et al. (2018). CESM1(WACCM) Stratospheric Aerosol Geoengineering Large Ensemble Project. Bulletin of the American Meteorological Society, 99(11), 2361–2371. https://doi.org/10.1175/BAMS-D-17-0267.1

https://doi.org/10.5194/egusphere-2026-3436
Preprint. Discussion started: 30 June 2026

Tilmes, S., MacMartin, D. G., Lenaerts, J. T. M., van Kampenhout, L., Muntjewerf, L., Xia, L., Harrison, C. S., Krumhardt, K. M., Mills, M. J., Kravitz, B., and Robock, A. (2020). Reaching 1.5 and 2.0 °C global surface temperature targets using stratospheric aerosol geoengineering, Earth Syst. Dynam., 11, 579–601, https://doi.org/10.5194/esd-11-579-2020

Trisos, C. H., Adelekan, I. O., Totin, E., Ayanlade, A., Efitre, J., et al. (2022). Africa. In: Climate Change 2022: Impacts, Adaptation, and Vulnerability. Contribution of Working Group II to the Sixth Assessment Report of the Intergovernmental Panel on Climate Change (pp. 1285–1455). Cambridge University Press.

Visioni, D., MacMartin, D.G., Kravitz, B., Boucher, O., Jones, A., Lurton, T., Martine, M., Mills, M.J., Nabat, P., Niemeier, U. and Séférian, R. (2021). Identifying the sources of uncertainty in climate model simulations of solar radiation modification with the G6sulfur and G6solar Geoengineering Model Intercomparison Project (GeoMIP) simulations. *Atmospheric Chemistry and Physics*, *21*(13), pp.10039-10063. https://doi.org/10.5194/acp-21-10039-2021